Pharmaceutical Research, Vol. 25, No. 11, November 2008 (© 2008)
DOI: 10.1007/s11095-008-9684-2

Research Paper

Can Ultrasound Solve the Transport Barrier of the Neural Retina?

Liesbeth Peeters,[1] Ine Lentacker,[1] Roosmarijn E. Vandenbroucke,[1] Bart Lucas,[1] Joseph Demeester,[1] Niek N. Sanders,[1] and Stefaan C. De Smedt[1,2]

Received March 4, 2008; accepted July 3, 2008; published online July 23, 2008

Purpose. Intravitreal injection of nonviral gene complexes may be promising in the treatment of retinal diseases. This study investigates the permeation of lipoplexes and polystyrene nanospheres through the neural retina and their uptake by the retinal pigment epithelium (RPE) either with or without ultrasound application.
Materials and Methods. Anterior parts and vitreous of bovine eyes were removed. The neural retina was left intact or peeled away from the RPE. (Non)pegylated lipoplexes and pegylated nanospheres were applied. After 2 h incubation, the RPE cells were detached and analyzed for particle uptake by flow cytometry and confocal microscopy.
Results. The neural retina is a significant transport barrier for pegylated nanospheres and (non)pegylated lipoplexes. Applying ultrasound improved the permeation of the nanoparticles up to 130 nm.
Conclusions. Delivery of liposomal DNA complexes to the RPE cells is strongly limited by the neural retina. Ultrasound energy may be a useful tool to improve the neural retina permeability, given the nucleic acid carriers are small enough. Our results underline the importance to design and develop very small carriers for the delivery of nucleic acids to the neural retina and the RPE after intravitreal injection.

KEY WORDS: lipoplexes; non viral gene therapy; ocular drug delivery; pegylation; ultrasound.

INTRODUCTION

The eye is an excellent candidate for gene therapy as it is easily accessible and immune-privileged. Moreover, many disease-causing mutations and their contribution to the pathogenesis of ocular diseases including cataracts, glaucoma and retinitis pigmentosa have been well characterized (1–5). In many cases, these ocular diseases are caused by a gene defect in the neural retina and/or the retinal pigment epithelium (RPE) cell layer (6,7). Since RPE integrity and function are (a) essential for neural retina homeostasis and (b) play a major role in both ocular diseases associated senescence [e.g. age related macular degeneration (AMD)] and in diseases associated with distrophies of the photoreceptors, the RPE is a promising target tissue for gene delivery (8).

Considerable progress has been made in the treatment of genetical ocular disorders using viral vectors, like recombinant-associated vectors (rAAV) and lentivirus-based vectors (9–11), as gene carriers. Perhaps the most spectacular result has been reported by Acland *et al.* (9) in the canine model of Leber Congenital Amaurosis. A single subretinal injection of rAAV vectors containing the healthy gene RPE65 was sufficient to restore retinal function and vision. Although viral gene therapy is very promising, the use of viral vectors has some important disadvantages like the limited size of the expression cassette, difficult large scale production and several safety issues like e.g. host immunity and oncogenesis (12–15). Therefore, nonviral gene carriers, based on lipids or polymers, remain interesting for ocular gene therapy.

Topical application and systemic administration are less suitable for the delivery of (non)viral gene particles to the retina and RPE. Indeed, the limited diffusion of nanoscopic particles through the sclera (16) after topical administration and the lack of extravasation into the eye after intraveneous administration [due to the tight blood-retina barrier (17)] do not allow an efficient delivery of drug loaded nanoparticles into the retina and the RPE. Therefore, in many cases, genetic vectors are administered through subretinal or intravitreal injection (18–23). Although subretinal injections are very efficient, this invasive and technical demanding technique is not always the first choice for treating ocular diseases, which are in general not life threatening (24). Intravitreal injections may form a clinically acceptable alternative. However, a major drawback is that the intravitreally injected vectors have to diffuse through the vitreous before they reach the retina. Moreover, if the gene carriers have to reach the RPE they also have to cross the neural retina.

Vitreous is a gel-like material that is built up of collagen fibrils bridged by proteoglycan filaments that contain negatively charged glycosaminoglycans (GAGs) (25). The interfibrillar spaces of this network are filled up by a dense network of hyaluronan (26). We and others showed that the biopolymer network in vitreous immobilizes nonviral gene complexes like lipoplexes (being nanoparticles composed of plasmid DNA and (cationic) lipids). Especially, the negatively charged

[1] Laboratory of General Biochemistry and Physical Pharmacy, Ghent University, Harelbekestraat 72, 9000 Ghent, Belgium.
[2] To whom correspondence should be addressed. (e-mail: Stefaan.Desmedt@UGent.be)

0724-8741/08/1100-2657/0 © 2008 Springer Science + Business Media, LLC

GAGs bind to the (positively charged) complexes which results in severe aggregation of the lipoplexes (27,28). We showed that aggregation of nanoparticles in vitreous can be circumvented by shielding their surface with polyethyleneglycol (PEG; named 'pegylation') (27,29).

Pegylation can thus avoid the aggregation of the vectors in the vitreous which also keeps them mobile in the vitreous. This is important as the vectors should finally reach the RPE. However, before they can reach the RPE they still have to cross the neural retina. Previous research by the Urtti group showed that the retina is poorly permeable for nonpegylated liposomal and polymeric gene complexes (28). The strongest barriers in the neuroretina seem to be the inner limiting membrane (ILM; Fig. 1A) and the interphotoreceptor matrix (IPRM; Fig. 1A). The ILM is the boundary region between the vitreous humor in the posterior chamber and the retina. It contains laminin, collagen and several proteoglycans (30). The ILM may be a sterical barrier for gene complexes while also interactions between the positively charged vectors and the negatively charged GAGs may take place which may immobilize the complexes and/or even release the nucleic acids prematurely (31). The IPRM, located between the outer limiting membrane of the retina and apical border of the RPE, also contains GAGs (32) and may thus also form a barrier for the penetrating gene complexes. Previously Pitkänen *et al*. (33) demonstrated that the passage of polyethyleneimine polyplexes, poly-L-lysine polyplexes and DOTAP liposomes through the neural retina was restricted by the ILM.

Application of ultrasound has been shown to enhance the transport of various drugs including macromolecules through tissues like the skin (34). A medium exposed to ultrasound experiences periodic pressure oscillations at a frequency and amplitude determined by the ultrasound source (35). Besides these pressure oscillations, the most significant secondary effect of ultrasound application, namely cavitation, can induce fluid velocities, shear forces and shock waves in the surrounding tissues (36,37). All the above mentioned effects transiently compromise the integrity of cell membranes or tissues, thereby achieving an enhanced uptake of applied molecules (35). Mesiwala *et al*. (38) reported that focused ultrasound can even induce reversible and non-destructive disruptions of the blood-brain barrier which may facilitate drug delivery to the brain. Ultrasound has also been used to enhance solute transport into the eye. Application of 880 kHz ultrasound significantly improved drug delivery through the cornea while causing only minor changes in the corneal eptithelium (39). Enhanced ocular drug delivery was also reported for glaucoma drugs using lower ultrasound frequencies (40).

In this work we used a bovine eye model to investigate to which extent the neural retina restricts the delivery of nonviral gene nanoparticles to the RPE. Firstly, as previous work showed that nonpegylated liposomal gene complexes do not penetrate the neural retina (28), we studied whether pegylation of lipoplexes improves their transport through the neural retina. Secondly, we investigated whether the size of the particles influences their mobility in the retinal tissue. Finally, as ultrasonic waves can enhance the penetration of drugs into the eye, we studied whether ultrasound energy may improve the transport of gene nanoparticles through the neural retina.

MATERIALS AND METHODS

Preparation of Cationic Lipoplexes

Preparation and Purification of Plasmid DNA

The pDNA used in this study was the pGL3-Control vector, consisting of 5,256 base pairs and containing as a reporter gene firefly luciferase under the control of a simian virus 40 promoter. The pDNA was amplified in *Escherichia coli* and purified as previously described (41). The pDNA concentration was set at 1.0 mg/ml in HEPES buffer (20 mM HEPES, pH 7.4) assuming that the absorption of 50 μg DNA/

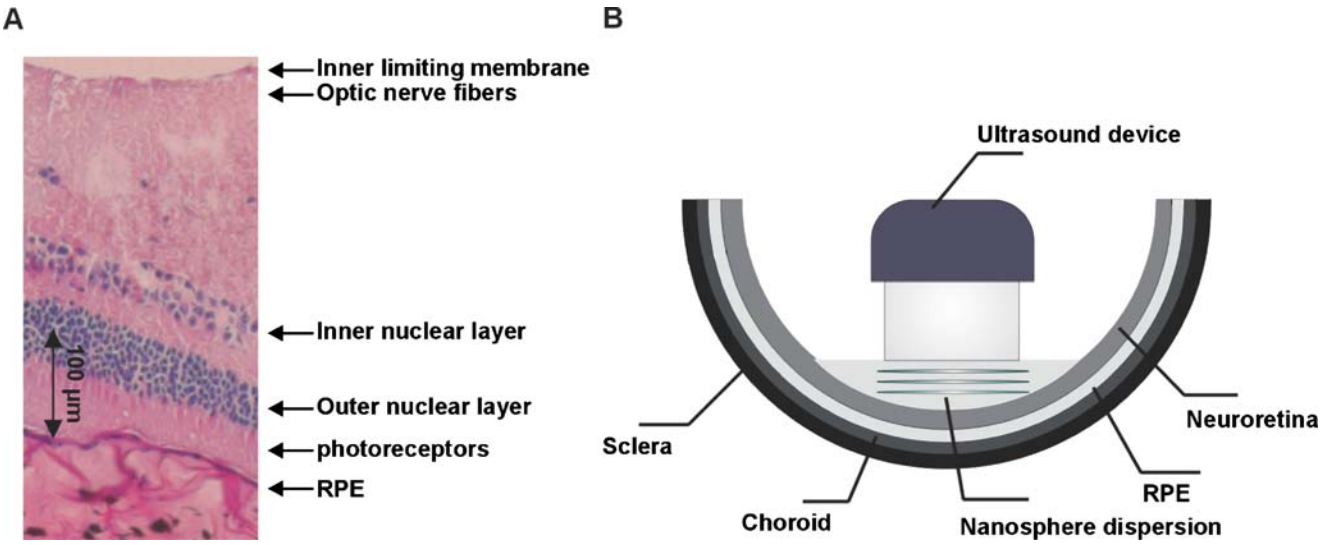

Fig. 1. **A** Microscopic image of the bovine retina shows the intact different layers of the retina after ultrasound exposure. **B** Overview of experimental setup with ultrasound device.

ml at 260 nm equals one. The pDNA solution showed a high purity as the 260/280 nm absorption ratio was between 1.8 and 2.0.

Preparation and Characterization of Cationic Liposomes

The phospholipids DOTAP (*N*-(1-(2,3-dioleoyloxy) propyl)-*N*,*N*,*N*-trimethylammoniumchloride), DOPE (dioleoyl-fosfatidylethanolamine) and DSPE-PEG (distearoyl-fosfatidylethanolamine-polyethyleneglycol) were purchased from Avanti Polar Lipids (Alabaster, AL, USA). To fluorescently label the liposomes cholesteryl Bodipy FLC12 (cholesteryl 4,4-difluoro-5,7-dimethyl-4-bora-3a,4a-diaza-*s*-indacene-3-dodecanoate) was used (Molecular Probes, Eugene, OR, USA).

Cationic liposomes containing the cationic lipid DOTAP and the neutral lipid DOPE in a 1:1 molar ratio with 0.1 mol % cholesteryl Bodipy FLC12 and 0, 4 and 17 mol% DSPE-PEG were prepared as previously described (40,41).

The weight-average hydrodynamic diameter of the cationic liposomes was determined by dynamic light scattering (DLS), using an Autosizer 4700 (Malvern, Worcestershire, UK). The zeta potential (ζ) was measured by determining the electrophoretic mobility using a Malvern Zeta-sizer 2000 (Malvern). For size and ζ measurements the cationic liposomes were dispersed in HEPES buffer (20 mM HEPES, pH 7.4). The average hydrodynamic diameter of the DOTAP/DOPE liposomes was 134±2 nm, 131±1 nm and 98±1 nm (mean±SD) for liposomes containing 0, 4, and 17 mol% DSPE-PEG respectively, while the zetapotential was 52±2, 23±3, and 15±1 mV respectively.

Preparation of Lipoplexes

Lipoplexes were prepared by mixing pDNA with cationic liposomes, containing 0 to 17 mol% DSPE-PEG, as described previously (41). Briefly, diluted pDNA (0.41 mg/ml) was added to an equal volume of cationic pegylated liposomes (5 mM DOTAP) resulting in a final +/− charge ratio of 4. Immediately after the addition of pDNA to the cationic pegylated liposomes, HEPES buffer was added until the final concentration of pDNA was 0.126 mg/ml. This mixture was then vortexed and incubated at room temperature for 30 min. The hydrodynamic diameter of the DOTAP/DOPE lipoplexes was 228±2, 203±5 and 115±1 nm for lipoplexes containing 0, 4, and 17 mol% DSPE-PEG, respectively. The zeta potential was 46±3, 15±2 and 1±1 mV, respectively.

Fluorescent Nanospheres

Fluorescent (yellow-green) polystyrene nanospheres (NS) of different sizes, bearing carboxyl groups at their surface, were purchased from Molecular Probes. The diameter and zeta potential of the nanospheres were measured as described above. The average hydrodynamic diameter of the nanospheres was 38±2, 122±5 and 190±7 nm respectively. The zeta potential of the nanospheres was −51±3, −42±2 and −46±3 mV, respectively.

The fluorescent polystyrene nanospheres described above were further coated with Pluronic F-127 (Sigma-Aldrich), a block-copolymer of polyethyleneglycol (PEG) and polypropylene oxide, as described before (41,42). Briefly, 150 µl of polystyrene nanospheres (sonificated during 10 min) were mixed with 850 µl distilled water and 2 ml of a Pluronic F-127 solution (10 mg/ml in distilled water). After vortexing, the nanospheres were incubated during 1 h at room temperature. Subsequently, 500 µl of the nanosphere suspension was transferred into a Microcon YM-100 centrifugal filter device (MWCO 100,000) (Millipore, Billerica, USA) and centrifuged during 12 min at 14,000×*g*. After centrifugation the concentrate with the Pluronic coated nanospheres was collected by placing the sample reservoir upside down in a new vial and spinning again 3 min at 1,000×*g*. The volume of the collected nanospheres was adjusted to 500 µl with HEPES buffer and the size and the zeta potential of the pluronic coated nanospheres were determined. The hydrodynamic diameter of the Pluronic coated nanospheres was 53±5, 131±4 and 218±7 nm (mean±SD) respectively. The zeta potential of the spheres was −15±8, −14±2, and −10±3 mV respectively. The nanospheres with diameter of 53, 131 and 218 nm are further referred to as NS53, NS131 and NS218, respectively.

Manipulation of Bovine Eyes

Fresh bovine eyes were obtained from a local abattoir and enucleated within half an hour after the animals had been slaughtered. The eyes were kept at +9°C. The eyes were treated as previously described by Pitkänen *et al*. (33) Briefly, after the eyes were cleaned of extra-ocular tissue and dipped in a 0.9% NaCl solution containing 1% penicillin/streptomycin (Gibco, Merelbeke, Belgium), they were opened circumferentially ±8 mm behind the limbus. The anterior tissues and the vitreous were separated gently from the neural retina. The neural retina was either left in its place or gently peeled and collected at the optic disc and cut with scissors near the optic nerve head. The optic nerve head was swept with a cotton swab to avoid blood cell contamination from cut vessels.

Transport of Lipoplexes and Polystyrene Nanospheres Through the Retina and Their Uptake by RPE Cells

The eyecups obtained as described above were set in the wells of a six-well-plate. Five hundred microliters of fluorescently labelled lipoplexes (containing 50 µg/ml pDNA) or nanospheres (1.5×10^{14} nanospheres per milliliter) were applied on the RPE or on the neural retina in the eye cups. After incubation of the eye cups (at 37°C during 2 to 4 h) with the lipoplexes/polystyrene nanospheres, the dispersion was removed and the surface was gently washed with 500 µl phosphate-buffered saline (PBS) (Gibco). The neural retina was subsequently carefully removed as described above. To collect the RPE cells, 500 µl of a 0.5% trypsine-EDTA solution (Gibco) was pipetted on the RPE surface, as described by Pitkänen *et al.* (33) After 1 to 2 min of incubation at room temperature, the RPE cells were brushed from the Bruch's membrane. Only the cells incubated under the surface of the trypsine solution were brushed.

To study the influence of ultrasound on the transport of the lipoplexes or nanospheres a sonitron 2000 (RichMar, Inola, OK, USA) equipped with a 22 mm probe was used. The probe made contact with the surface of the lipoplex/

nanosphere dispersion as illustrated in Fig. 1B. The following ultrasound settings were applied: (a) a frequency of 1 MHz was used in all experiments, (b) a 50% or 100% duty cycle was applied, (c) the ultrasound intensity was 0.5 or 1 W/cm^2 while (d) the radiation times were 30, 60 or 120 s.

Confocal Microscopy on the RPE Cells

For imaging the RPE cells by confocal microscopy, the RPE cells collected as described above were immediately diluted with 500 µl of Dulbecco's modified Eagle's medium (DMEM) containing 2 mM glutamine, 10% heat deactivated fetal bovine serum (FBS), penicillin (100 U/ml) and streptomycin (100 µg/ml). All the culture reagents were obtained from Gibco. The cells were centrifuged during 10 min at 6000 rpm (Beckman Coulter Microfuge 18) and subsequently the cell pellet was resuspended in DMEM. 200 µl of this dispersion was seeded on a glass-bottomed cover slip (MatTek Corporation, Ashland, USA) and incubated during 2 to 3 h at 37°C in a humified atmosphere containing 5% CO_2. After the incubation, the cell membranes were labeled with Concanavalin A Alexa Fluor 647 as described by the manufacturer (Molecular Probes). The samples were visualized on a Nikon C1si confocal laser scanning module attached to a motorized Nikon TE2000-E inverted microscope (Nikon Benelux, Brussels, Belgium) with a 60× water immersion objective using the 561 and 647 nm laser line for excitation. A non-confocal diascopic DIC (differential interference contrast) image was collected simultaneously with the confocal images.

Analysis of the RPE Cells by Flow Cytometry

For flow cytometry (FACS) analysis, the RPE cells, collected as described above, were immediately fixed with 1% paraformaldehyde and centrifuged at 6,000 rpm for 10 min (Beckman Coulter Microfuge 18). For removal of the contaminants the cells were suspended in 2 ml of 0.32 M sucrose/50 mM phosphate buffer (pH 7.2) and centrifuged during 10 min at 2,000 rpm (Beckman Coulter Microfuge 18). The supernatant was carefully removed and the centrifugation in buffered sucrose was repeated twice. Microscopy images revealed that after centrifugation in sucrose the samples contained mainly RPE cells, but occasionally some outer segment fragments, erythrocytes, and pigment granules were still present. After the last centrifugation in sucrose, the pellet was washed with 1% paraformaldehyde, centrifuged during 10 min at 6,000 rpm (Beckman Coulter Microfuge 18) and diluted to 500 µl with 1% paraformaldehyde.

A Beckman Coulter Cytomics FC 500 5 colour flow cytometer, equipped with a 488 nm argon ion laser, was used. For each sample, a minimum of 10,000 events was collected. The cells were visualized on an FSC (forward scattering) *versus* SSC (side scattering at 90°) display. The RPE cells that were living before fixation were selected for analysis by gating. The dead RPE cells and the possible remaining erythrocytes, photoreceptor outer segments and pigment granules were excluded on the basis of their size and other scattering properties.

In evaluating the FACS data obtained from the RPE cells from the left eye of a cow (which was treated with lipoplexes/nanospheres) the FACS results obtained from the RPE cells from the right eye of the same cow (which was not treated with lipoplexes/nanospheres) were used as 'blanco'. The gate for each blanc sample was adjusted so that the percentage of fluorescent RPE cells (positive events) was around 2%.

To evaluate the influence of ultrasound on the permeation of the fluorescent polystyrene nanospheres through the retina, the FACS results obtained from RPE cells isolated from the left eye of a cow (which received nanospheres and ultrasound energy) were compared with the FACS results obtained from the RPE cells isolated from the right eye of the same cow which also received polystyrene nanospheres but no ultrasound energy (blanco). The gate for each blanc sample was again set so that the percentage of fluorescent RPE cells (positive events) was around 2%.

All FACS experiments were repeated three times at least, which means the analysis of at least three pairs of bovine eyes per tested particle.

Statistical Analysis

The Mann–Whitney *U* test was used for statistical analysis of the FACS results. A value of $P<0.05$ was considered significant.

Histological Analysis

After incubation of the eye cups (at 37°C during 2 h) with the lipoplexes/polystyrene nanospheres, the dispersion was removed and the surface was gently washed with 500 µl phosphate-buffered saline. The samples were frozen in Tissue-Tek O.C.T compound (Sakura, Torrance, CA, USA) and cryostat cuts of 5 µm were prepared. The samples were visualized on a TS100F Nikon fluorescence inverted microscope.

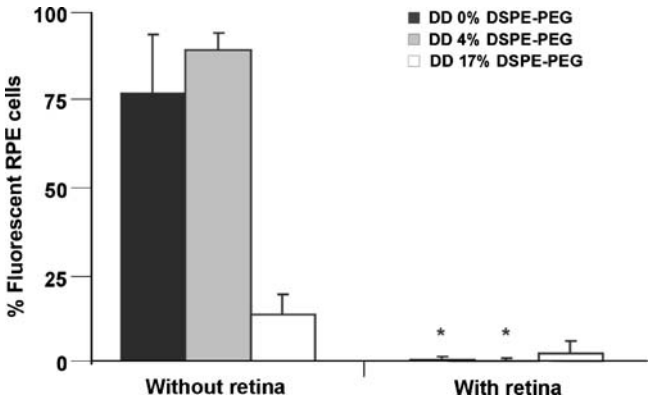

Fig. 2. Percentage of fluorescent RPE cells after application of non-pegylated and pegylated DOTAP DOPE lipoplexes respectively on the RPE cells ('without retina') or on the neural retina covering the RPE ('with retina'). Means±SD are shown ($n=3$). The uptake of DD 0% DSPE-PEG and DD 4% DSPE-PEG by the RPE cells decreased significantly ($P<0.05$) when the lipoplexes were applied on the neural retina compared with the situation were the lipoplexes were applied directly on the RPE cell layer.

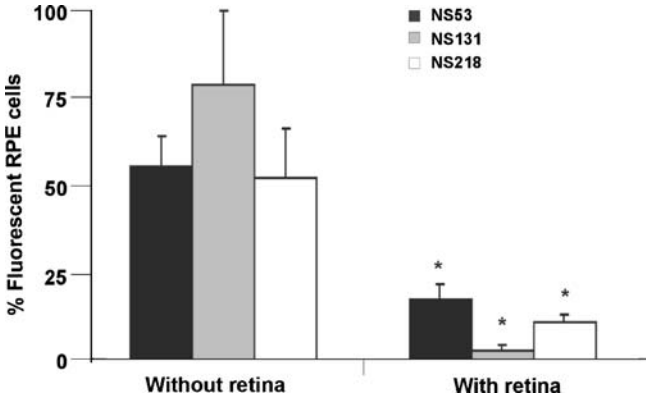

Fig. 3. Percentage of fluorescent RPE cells after application of pegylated polystyrene nanospheres respectively on the RPE cells ('without retina') or on the neural retina covering the RPE ('with retina'). Means±SD are shown (n=4 to 5). The RPE cell uptake of all tested nanospheres decreased significantly (P<0.05) when the nanospheres were applied on the neural retina compared with the situation were the nanospheres were applied directly on the RPE cell layer.

RESULTS

Influence of the Neural Retina on the Uptake of Lipoplexes and Polystyrene Nanospheres by RPE Cells

The FACS analysis revealed that, in case the neural retina was removed from the RPE cells in the eye cups, 78% of the RPE cells took up nonpegylated lipoplexes (DD 0% DSPE-PEG). When these lipoplexes were delivered on the neural retina covering the RPE, only 1% of the RPE cells seemed to contain lipoplexes (Fig. 2). We observed similar findings for the lowly pegylated lipolexes (4% DSPE-PEG; Fig. 2). The uptake of highly pegylated lipoplexes (17% DSPE-PEG) by the RPE cells not covered with neural retina was substantionally lower when compared to the non-pegylated and the 4% pegylated lipoplexes (Fig. 2). The retina also seemed to lower the uptake of these highly pegylated lipoplexes by RPE cells, though the decrease was not significant.

Figure 3 shows that, in case the RPE cells were not covered by the neural retina, about 55%, 78%, and 52% of the RPE cells took up NS53 (53 nm), NS131 (131 nm) and NS218 (218 nm) pegylated polystyrene nanospheres, respectively. When the nanospheres were applied on the neural retina, the uptake lowered to 17%, 3% and 11% for NS53, NS131 and NS218 nanospheres, respectively.

To confirm the outcome of the FACS experiments the RPE cells were investigated by confocal microscopy. The confocal images confirmed the presence of fluorescent polystyrene nanospheres in the RPE cells only when the nanospheres were directly applied on the RPE cell layer (Fig. 4C). RPE cells that were covered by the neural retina did not take up nanospheres (Fig. 4B).

Fluorescence microscopy on the neural retina (Fig. 5) also confirmed that only few of the pegylated nanospheres penetrated into the retina. They could be seen in the layer of the optic nerve fibres. We should note, however, that localization of the pegylated polystyrene nanospheres in the retinal tissues by microscopy was not straightforward due to both the small size/low number of the penetrating particles and the autofluorescence of the retinal tissue.

Influence of Ultrasound on the Uptake of Fluorescent Nanospheres by RPE Cells Covered with a Neural Retina

With the aim to improve the penetration of the fluorescent nanospheres through the neural retina, and thus to enhance the uptake by RPE cells, ultrasound energy was applied as illustrated in Fig. 1B.

Figure 6 shows that ultrasound energy significantly improves the uptake of fluorescent NS53 nanospheres by RPE cells covered with neural retina which is, most probable, attributed to a better penetration through the neural retina. Even the mildest ultrasound condition (DC100%, 0.5 W/cm^2, 30 s) increased the percentage of NS53 positive RPE cells up to

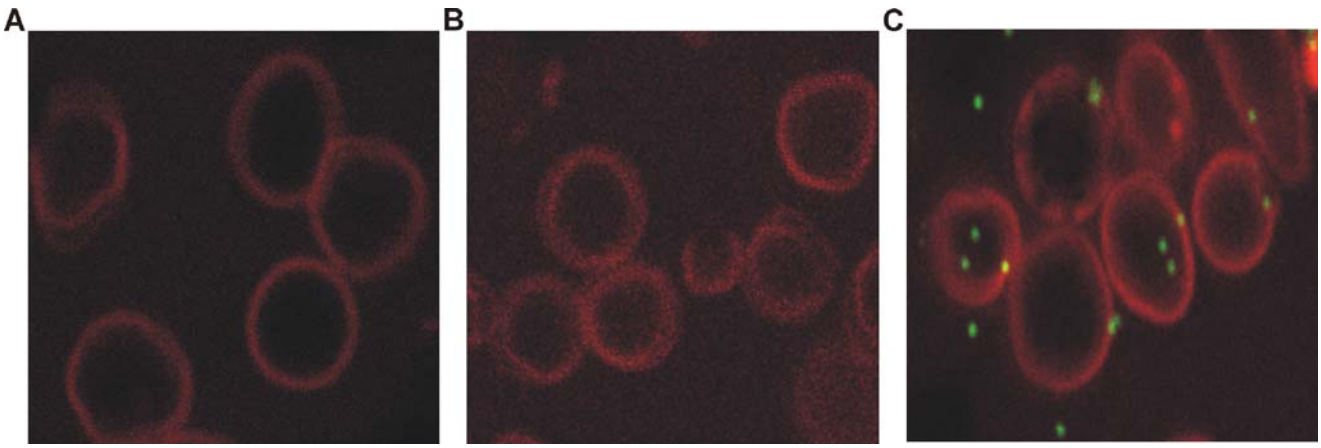

Fig. 4. Confocal images of RPE cells. The cellular membranes are coloured in red, while the pegylated polystyrene nanospheres are green. When pegylated polystyrene nanospheres were applied on the neural retina covering the RPE, nanospheres were not detected in the RPE cells (**B**). In contrast, RPE cells containing pegylated polystyrene spheres were seen in case the nanospheres were directly applied on the RPE cells (**C**). Panel **A** shows isolated RPE cells of a blanc sample.

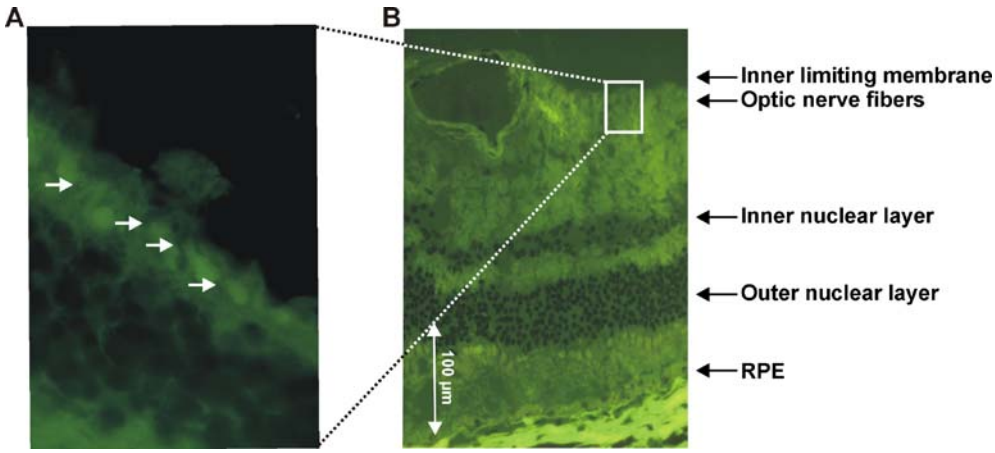

Fig. 5. **A** Localisation of 100 nm polystyrene spheres in the optic nerve layer. **B** Overview picture of the retina.

17 times, when compared to the outcome of the experiments without use of ultrasound. Applying ultrasound for longer times (60 s instead of 30 s) did not further increase the percentage of NS53 positive RPE cells (data not shown).

Applying ultrasound during 30 s did not increase the uptake of the larger NS131 fluorescent nanospheres by the RPE cells. Only after 2 min of ultrasound irradiation a statistically significant increase in NS131 positive RPE cells was observed (Fig. 6).

Applying ultrasound, even during 2 min, did not increase the uptake of the NS218 fluorescent nanospheres by the RPE cells, being the largest polystyrene nanospheres used in this study. Applying ultrasound for longer than 2 min was not an option as the retina became (even visibly) damaged.

To check the condition of the neural retina after application of ultrasound, cryocoupes were prepared and studied by microscopy. Figure 1A suggests that the ultrasound energy did not influence the integrity of the retinal tissue.

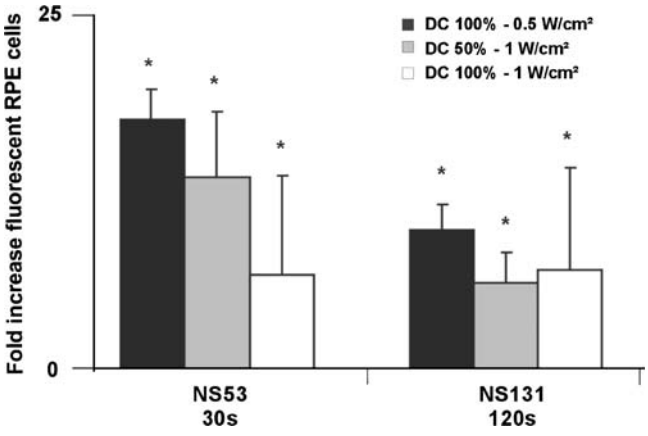

Fig. 6. Fold increase in fluorescent RPE cells by using ultrasound energy. The pegylated polystyrene nanospheres were applied on the neural retina covering the RPE.The x-axis indicates both which nanospheres were used and the duration of ultrasound exposure. Means±SD are shown (n=3). The RPE cell uptake of the NS53 and NS131 increased significantly (P<0.05) when ultrasound energy was applied. This indicates an increased permeation through the neural retina.

DISCUSSION

Since genetic defects in RPE cells can drastically impair the normal visual function, RPE cells are interesting target cells for ocular gene therapy. A major difficulty in the genetic treatment of RPE cells is their limited accessibility. Due to the blood-retina barrier, systemical application of gene therapy complexes is excluded (17). Subretinal or intravitreal injection are possible routes of administration for gene complexes. Subretinal injection, however, is a very invasive technique (24), so intravitreal injection is probably the best alternative method. However, after intravitreal injection, the administered vectors must permeate through the vitreous and neural retina to reach the RPE. Understanding these biological barriers should provide us with background information necessary to design efficient nonviral vectors for retinal gene therapy by intravitreal injection. However, there is very sparse information available on both the biological barriers nonviral gene complexes have to overcome after intravitreal injection and the biological mechanisms in the RPE which determine the fate, and thus the transfection efficiency, of nonviral gene complexes in RPE cells.

Figure 2 shows that primary RPE cells efficiently internalize non-pegylated and lowly pegylated lipoplexes (4% DSPE-PEG), provided they are directly administered to the surface of the PRE cells. Clearly, the uptake of highly pegylated lipoplexes (17% DSPE-PEG) occurs to a much lesser extent. This result is in agreement with our previous studies in which we used an *in vitro* RPE cell line (D407 RPE cells), which showed that highly pegylated lipoplexes were poorly transfecting the RPE cells. Confocal images showed that these lipoplexes became entrapped in the endosomal pathway and eventually were degradated in the lysosomes, which explains their low transfection efficiency (29).

Previous research of our group showed that in vitreous nonpegylated and lowly pegylated lipoplexes seriously aggregate which immobilizes them in the vitreous gel (28,42). The

aggregation is due to interactions between the positively charged nonpegylated and lowly pegylated lipoplexes and the negatively charged GAGs present in the vitreous. Only by covering the surface of the lipoplexes with sufficient amounts of PEG, which renders the lipoplexes less positive, we could avoid this aggregation. Unfortunately, in contrast to the situation in vitreous, we show in this study that a high pegylation degree of DOTAP DOPE lipoplexes does not improve their permeation through the neural retina. Our results confirm previous experiments by Pitkänen *et al.* (33) who found that neural retina completely blocks nonpegylated lipoplexes. Their data indicated that the cationic charge of the penetrating substance is even more important than its size. As an example, FITC-dextrans (20,000 g/mol) permeated the retina well, while positively charged FITC-PLL chains of a similar size became practically blocked.

To get a better view on the role of the size of substances permeating through the neural retina we used polystyrene nanospheres. We previously showed that negatively charged carboxylated spheres attach to the vitreous network (42). We could overcome this by pegylating the nanospheres through coating with Pluronic F-127. As Fig. 3 shows, such pegylated polystyrene nanospheres are internalized quite efficiently by the primary RPE cells when they are in direct contact. However, the neural retina blocks even the smallest pegylated polystyrene nanospheres (NS53) significantly. We would like to remark that our experiments were done post mortem and thus we cannot exclude possible metabolic differences compared with the *in vivo* situation. However, in agreement with our results, Farjo *et al.* (43) showed that after intravitreal injection in mice of compacted DNA nanoparticles with an average minor diameter of 18 nm, EFGP expression was high in the lens, but the expression levels in the pigment epithelium cells and retina were a multi-fold lower than those observed in the lens. These *in vivo* results also indicate that the neural retina forms a real barrier even for very small and neutral gene therapy complexes. Moreover, Jackson *et al.* determined the maximum size of molecules capable of freely diffusing across the retina *in vitro* and concluded that the retinal exclusion limit is around 7 nm (44). In contrast, other research groups reported gene transfer in RPE cells of rats, albeit at relatively low levels, after intravitreal injection of lipoplexes suggesting that lipoplexes should be able to move through retina (45,46).

It has been shown that ultrasound energy enhances tissue permeability, like e.g. the permeability of the skin (34). Moreover, low frequency sonophoresis is now widely used for clinical examinations and therapies and its safety has been reliably established. Previous research showed that gene transfer to the ocular surface can be improved by using ultrasound technology (47,48). Therefore we investigated whether ultrasound energy may improve the permeability of the neural retina. Fluorescence microscopy images showed that the ultrasound waves as applied in the experiments did not cause visible tissue damage (Fig. 1A). As Fig. 6 shows, the permeation of the small polystyrene nanoparticles (NS53) through the retina could be significantly improved by rather gentle ultrasound conditions (30 s 0.5 W/cm^2 1 MHz DC 100%). In contrast, significantly longer radiation times were necessary to significantly improve the permeation of the larger polystyrene nanospheres (NS131) through the neural retina. The permeation of the largest nanospheres used in this study (NS218) could not be improved by the given ultrasound conditions. However, one should take into account that the distance between the ultrasound source and the neural retina *in vivo* will be larger than in the experimental set up of our study. Moreover, other tissues like e.g. cornea and lens may absorb a part of the ultrasound energy thereby decreasing the intensity that can act on the neural retina.

In this study, we tried to improve the penetration of nanoparticles through the neural retina by ultrasound. Other studies tested the influence of ultrasound on the gene expression efficiency (49,50). Although they found an ultrasound related improvement of the transfection efficiency, our study on RPE cells (unpublished data) showed no significant improvement of the transfection efficiency with (pegylated) DOTAP DOPE lipoplexes. This was in agreement with other results generated by our group (51,52). Lipoplex mediated gene transfer could only be improved by coupling the lipoplexes to ultrasound responsive microbubbles. In our opinion however, the ocular applicability of these microbubbles is quite insure due to their relative large size (between 0.5 and 10 μm). Moreover, implosion of these bubbles during ultrasound exposure generates shock-waves and microjets causing cell membrane perforations.

One could expect that the main permeation barriers in the neural retina are the interphotoreceptor matrix (IPRM) and the inner limiting membrane (ILM). The fluorescence microscopy images in Fig. 5 suggest that the ILM seems to restrict the passage of the nanospheres as only few particles could reach the optic nerve layer just underneath the ILM. This is in agreement with the results of Pitkänen *et al.* (33) who suggested that GAGs present in the ILM may be (a) a mechanical barrier and (b) the GAGs in the ILM may also interact with the penetrating particles which may lead to immobilization.

On the one hand our results show that RPE cells are quite efficient in internalizing (non)pegylated DOTAP DOPE lipoplexes and polystyrene nanospheres of different sizes. This is in agreement with the fact that RPE cells are active phagocyting cells, as they are responsible for the phagocytosis and subsequent digestion of the photoreceptor outer segments (53). On the other hand, the neural retina seems to form an important barrier for lipoplexes and nanospheres. Ultrasound energy could be a useful tool to improve the neural retina permeability, though the improvement of the permeation seems to be restricted to rather small particles. Our results underline the importance to design and develop very small carrier for the delivery of nucleic acids to the neural retina and the RPE.

ACKNOWLEDGMENTS

This work was supported by a grant from the Fund for Research in Ophthalmology Belgium. The post-doctoral fellowship of N.N. Sandres is supported by the Fund for Scientific Research (FWO). The authors like to thank Caroline Vandenbroecke, Christophe Delaye, Bart Leroy and Jan Philippé for their contribution. We acknowledge Ghent University (BOF) and FP7 of the European Union for financial support.

REFERENCES

1. V. Berry, P. Francis, S. Kaushal, A. Moore, and S. Bhattacharya. Missense mutations in MIP underlie autosomal dominant 'polymorphic' and lamellar cataracts linked to 12q. *Nat. Genet.* **25**:15–17 (2000). doi:10.1038/75538.
2. E. M. Stone, J. H. Fingert, W. L. Alward, T. D. Nguyen, J. R. Polansky, S. L. Sunden, D. Nishimura, A. F. Clark, A. Nystuen, B. E. Nichols, D. A. Mackey, R. Ritch, J. W. Kalenak, E. R. Craven, and V. C. Sheffield. Identification of a gene that causes primary open angle glaucoma. *Science.* **275**:668–670 (1997). doi:10.1126/science.275.5300.668.
3. G. J. Farrar, P. F. Kenna, and P. Humphries. On the genetics of retinitis pigmentosa and on mutation-independent approaches to therapeutic intervention. *EMBO J.* **21**:857–864 (2002). doi:10.1093/emboj/21.5.857.
4. P. A. Ferreira. Insights into X-linked retinitis pigmentosa type 3, allied diseases and underlying pathomechanisms. *Hum. Mol. Genet.* **14**(Spec No. 2):R259–R267 (2005).
5. R. S. Molday. Photoreceptor membrane proteins, phototransduction, and retinal degenerative diseases. The Friedenwald Lecture. *Invest. Ophthalmol. Vis. Sci.* **39**:2491–2513 (1998).
6. P. A. Campochiaro. Retinal and choroidal neovascularization. *J. Cell. Physiol.* **184**:301–310 (2000). doi:10.1002/1097-4652(200009)184:3<301::AID-JCP3>3.0.CO;2-H.
7. R. S. Molday. Photoreceptor membrane proteins, phototransduction, and retinal degenerative diseases. The Friedenwald Lecture. *Invest. Ophthalmol. Vis. Sci.* **39**:2491–2513 (1998).
8. R. A. Bejjani, D. BenEzra, H. Cohen, J. Rieger, C. Andrieu, J. C. Jeanny, G. Gollomb, and F. F. Behar-Cohen. Nanoparticles for gene delivery to retinal pigment epithelial cells. *Mol. Vis.* **11**:124–132 (2005).
9. G. M. Acland, G. D. Aguirre, J. Ray, Q. Zhang, T. S. Aleman, A. V. Cideciyan, S. E. Pearce-Kelling, V. Anand, Y. Zeng, A. M. Maguire, S. G. Jacobson, W. W. Hauswirth, and J. Bennett. Gene therapy restores vision in a canine model of childhood blindness. *Nat. Genet.* **28**:92–95 (2001). doi:10.1038/88327.
10. G. M. Acland, G. D. Aguirre, J. Bennett, T. S. Aleman, A. V. Cideciyan, J. Bennicelli, N. S. Dejneka, S. E. Pearce-Kelling, A. M. Maguire, K. Palczewski, W. W. Hauswirth, and S. G. Jacobson. Long-term restoration of rod and cone vision by single dose rAAV-mediated gene transfer to the retina in a canine model of childhood blindness. *Mol. Ther.* **12**:1072–1082 (2005). doi:10.1016/j.ymthe.2005.08.008.
11. J. W. Bainbridge, M. H. Tan, and R. R. Ali. Gene therapy progress and prospects: the eye. *Gene Ther.* **13**:1191–1197 (2006). doi:10.1038/sj.gt.3302812.
12. C. Baum, O. Kustikova, U. Modlich, Z. Li, and B. Fehse. Mutagenesis and oncogenesis by chromosomal insertion of gene transfer vectors. *Hum. Gene Ther.* **17**:253–263 (2006). doi:10.1089/hum.2006.17.253.
13. C. L. Halbert, A. D. Miller, S. McNamara, J. Emerson, R. L. Gibson, B. Ramsey, and M. L. Aitken. Prevalence of neutralizing antibodies against adeno-associated virus (AAV) types 2, 5, and 6 in cystic fibrosis and normal populations: Implications for gene therapy using AAV vectors. *Hum. Gene Ther.* **17**:440–447 (2006). doi:10.1089/hum.2006.17.440.
14. S. E. Raper, N. Chirmule, F. S. Lee, N. A. Wivel, A. Bagg, G. P. Gao, J. M. Wilson, and M. L. Batshaw. Fatal systemic inflammatory response syndrome in a ornithine transcarbamylase deficient patient following adenoviral gene transfer. *Mol. Genet Metab.* **80**:148–158 (2003). doi:10.1016/j.ymgme.2003.08.016.
15. C. E. Thomas, A. Ehrhardt, and M. A. Kay. Progress and problems with the use of viral vectors for gene therapy. *Nat. Rev. Genet.* **4**:346–358 (2003). doi:10.1038/nrg1066.
16. R. N. Weinreb. Enhancement of scleral macromolecular permeability with prostaglandins. *Trans. Am. Ophthalmol. Soc.* **99**:319–343 (2001).
17. S. Duvvuri, S. Majumdar, and A. K. Mitra. Drug delivery to the retina: challenges and opportunities. *Expert Opin. Biol. Ther.* **3**:45–56 (2003). doi:10.1517/14712598.3.1.45.
18. J. Bennett, A. M. Maguire, A. V. Cideciyan, M. Schnell, E. Glover, V. Anand, T. S. Aleman, N. Chirmule, A. R. Gupta, Y. Huang, G. P. Gao, W. C. Nyberg, J. Tazelaar, J. Hughes, J. M. Wilson, and S. G. Jacobson. Stable transgene expression in rod photoreceptors after recombinant adeno-associated virus-mediated gene transfer to monkey retina. *Proc. Natl. Acad. Sci. U S A.* **96**:9920–9925 (1999). doi:10.1073/pnas.96.17.9920.
19. A. R. Harvey, W. Kamphuis, R. Eggers, N. A. Symons, B. Blits, S. Niclou, G. J. Boer, and J. Verhaagen. Intravitreal injection of adeno-associated viral vectors results in the transduction of different types of retinal neurons in neonatal and adult rats: a comparison with lentiviral vectors. *Mol. Cell Neurosci.* **21**:141–157 (2002). doi:10.1006/mcne.2002.1168.
20. H. Miyoshi, M. Takahashi, F. H. Gage, and I. M. Verma. Stable and efficient gene transfer into the retina using an HIV-based lentiviral vector. *Proc. Natl. Acad. Sci. U S A.* **94**:10319–10323 (1997). doi:10.1073/pnas.94.19.10319.
21. G. M. Sarra, C. Stephens, F. C. Schlichtenbrede, J. W. B. Bainbridge, A. J. Thrasher, P. J. Luthert, and R. R. Ali. Kinetics of transgene expression in mouse retina following sub-retinal injection of recombinant adeno-associated virus. *Vis. Res.* **42**:541–549 (1901). doi:10.1016/S0042-6989(01)00230-9.
22. G. M. Sarra, C. Stephens, M. de-Alwis, J. W. Bainbridge, A. J. Smith, A. J. Thrasher, and R. R. Ali. Gene replacement therapy in the retinal degeneration slow (rds) mouse: the effect on retinal degeneration following partial transduction of the retina. *Hum. Mol. Genet.* **10**:2353–2361 (2001). doi:10.1093/hmg/10.21.2353.
23. M. Takahashi, K. Miyoshi, I. M. Verma, and F. H. Gage. Rescue from photoreceptor degeneration in the rd mouse by human immunodeficiency virus vector-mediated gene transfer. *J. Virol.* **73**:7812–7816 (1999).
24. T. Sakamoto, Y. Ikeda, and Y. Yonemitsu. Gene targeting to the retina. *Adv. Drug Deliv. Rev.* **52**:93–102 (2001). doi:10.1016/S0169-409X(01)00191-0.
25. P. Bishop. The biochemical structure of mammalian vitreous. *Eye.* **10**:664–670 (1996).
26. J. E. Scott. The chemical morphology of the vitreous. *Eye.* **6**:553–555 (1992).
27. L. Peeters, N. N. Sanders, K. Braeckmans, K. Boussery, V. d. Van, S. C. De Smedt, and J. Demeester. Vitreous: a barrier to nonviral ocular gene therapy. *Invest. Ophthalmol. Vis. Sci.* **46**:3553–3561 (2005). doi:10.1167/iovs.05-0165.
28. L. Pitkanen, M. Ruponen, J. Nieminen, and A. Urtti. Vitreous is a barrier in nonviral gene transfer by cationic lipids and polymers. *Pharm. Res.* **20**:576–583 (2003). doi:10.1023/A:1023238530504.
29. L. Peeters, N. N. Sanders, A. Jones, J. Demeester, and S. C. De Smedt. Post-pegylated lipoplexes are promising vehicles for gene delivery in RPE cells. *J. Control Release.* **121**:208–217 (2007). doi:10.1016/j.jconrel.2007.05.033.
30. S. R. Russell, J. D. Shepherd, and G. S. Hageman. Distribution of glycoconjugates in the human retinal internal limiting membrane. *Invest. Ophthalmol. Vis. Sci.* **32**:1986–1995 (1991).
31. M. Ruponen, H. S. Yla, and A. Urtti. Interactions of polymeric and liposomal gene delivery systems with extracellular glycosaminoglycans: physicochemical and transfection studies. *Biochim. Biophys. Acta Biomembr.* **1415**:331–341 (1999). doi:10.1016/S0005-2736(98)00199-0.
32. G. S. Hageman, and L. V. Johnson. Chondroitin 6-sulfate glycosaminoglycan is a major constituent of primate cone photoreceptor matrix sheaths. *Curr. Eye Res.* **6**:639–646 (1987). doi:10.3109/02713688709025225.
33. L. Pitkanen, J. Pelkonen, M. Ruponen, S. Ronkko, and A. Urtti. Neural retina limits the nonviral gene transfer to retinal pigment epithelium in an *in vitro* bovine eye model. *AAPS J.* **6**:e25 (2004). doi:10.1208/aapsj060325.
34. S. Mitragotri, and J. Kost. Low-frequency sonophoresis: a review. *Adv. Drug Deliv. Rev.* **56**:589–601 (2004). doi:10.1016/j.addr.2003.10.024.
35. S. Mitragotri. Healing sound: the use of ultrasound in drug delivery and other therapeutic applications. *Nat. Rev. Drug Discov.* **4**:255–260 (2005). doi:10.1038/nrd1662.
36. R. Pecha, and B. Gompf. Microimplosions: cavitation collapse and shock wave emission on a nanosecond time scale. *Phys. Rev. Lett.* **84**:1328–1330 (2000). doi:10.1103/PhysRevLett.84.1328.
37. K. S. Suslick. Ultrasound: Its Chemical, Physical and Biological Effects. VCH, New York, 19882008. Ref Type: Generic.

38. A. H. Mesiwala, L. Farrell, H. J. Wenzel, D. L. Silbergeld, L. A. Crum, H. R. Winn, and P. D. Mourad. High-intensity focused ultrasound selectively disrupts the blood-brain barrier *in vivo*. *Ultrasound. Med. Biol.* **28**:389–400 (2002). doi:10.1016/S0301-5629(01)00521-X.
39. V. Zderic, J. I. Clark, and S. Vaezy. Drug delivery into the eye with the use of ultrasound. *J. Ultrasound. Med.* **23**:1349–1359 (2004).
40. V. Zderic, S. Vaezy, R. W. Martin, and J. I. Clark. Ocular drug delivery using 20-kHz ultrasound. *Ultrasound. Med. Biol.* **28**:823–829 (2002). doi:10.1016/S0301-5629(02)00515-X.
41. N. N. Sanders, E. Van Rompaey, S. C. De Smedt, and J. Demeester. Structural alterations of gene complexes by cystic fibrosis sputum. *Am. J. Respir. Crit. Care Med.* **164**:486–493 (2001).
42. L. Peeters, N. N. Sanders, K. Braeckmans, K. Boussery, V. d. Van, S. C. De Smedt, and J. Demeester. Vitreous: a barrier to nonviral ocular gene therapy. *Invest. Ophthalmol. Vis. Sci.* **46**:3553–3561 (2005). doi:10.1167/iovs.05-0165.
43. R. Farjo, J. Skaggs, A. B. Quiambao, M. J. Cooper, and M. I. Naash. Efficient non-viral ocular gene transfer with compacted DNA nanoparticles. *PLoS One.* **1**:e38 (2006). doi:10.1371/journal.pone.0000038.
44. T. L. Jackson, R. J. Antcliff, J. Hillenkamp, and J. Marshall. Human retinal molecular weight exclusion limit and estimate of species variation. *Invest. Ophthalmol. Vis. Sci.* **44**:2141–2146 (2003). doi:10.1167/iovs.02-1027.
45. M. Hangai, Y. Kaneda, H. Tanihara, and Y. Honda. *In vivo* gene transfer into the retina mediated by a novel liposome system. *Invest. Ophthalmol. Vis. Sci.* **37**:2678–2685 (1996).
46. I. Masuda, T. Matsuo, T. Yasuda, and N. Matsuo. Gene transfer with liposomes to the intraocular tissues by different routes of administration. *Invest. Ophthalmol. Vis. Sci.* **37**:1914–1920 (1996).
47. S. Sonoda, K. Tachibana, E. Uchino, A. Okubo, M. Yamamoto, K. Sakoda, T. Hisatomi, K. H. Sonoda, Y. Negishi, Y. Izumi, S. Takao, and T. Sakamoto. Gene transfer to corneal epithelium and keratocytes mediated by ultrasound with microbubbles. *Invest. Ophthalmol. Vis. Sci.* **47**:558–564 (2006). doi:10.1167/iovs.05-0889.
48. T. Yamashita, S. Sonoda, R. Suzuki, N. Arimura, K. Tachibana, K. Maruyama, and T. Sakamoto. A novel bubble liposome and ultrasound-mediated gene transfer to ocular surface: RC-1 cells *in vitro* and conjunctiva *in vivo*. *Exp. Eye Res.* **85**:741–748 (2007). doi:10.1016/j.exer.2007.08.006.
49. L. B. Feril Jr., R. Ogawa, H. Kobayashi, H. Kikuchi, and T. Kondo. Ultrasound enhances liposome-mediated gene transfection. *Ultrason. Sonochem.* **12**:489–493 (2005). doi:10.1016/j.ultsonch.2004.06.006.
50. E. C. Unger, T. P. McCreery, and R. H. Sweitzer. Ultrasound enhances gene expression of liposomal transfection. *Invest. Radiol.* **32**:723–727 (1997). doi:10.1097/00004424-199712000-00001.
51. I. Lentacker, S. De Smedt, J. Demeester, V. Van Marck, M. Bracke, and N. Sanders. Lipoplex-loaded microbubbles for gene delivery: A Trojan horse controlled by ultrasound. *Hum. Gene Ther.* **18**:1046 (2007).
52. R. E. Vandenbroucke, I. Lentacker, J. Demeester, S. C. De Smedt, and N. N. Sanders. Ultrasound assisted siRNA delivery using PEG-siPlex loaded microbubbles. *J. Control Release.* **126**:265–273 (2008). doi:10.1016/j.jconrel.2007.12.001.
53. O. Strauss. The retinal pigment epithelium in visual function. *Physiol. Rev.* **85**:845–881 (2005). doi:10.1152/physrev.00021.2004.